Table 1 Most common signs and symptoms in patients with AADC deficiency

Symptoms[a]	%	All patients	Infancy, ≤18 mo	Childhood, ≤10 y	Adolescence, ≥11 y	Adulthood
Characteristic features						
Hypotonia	95	74/78	35/38	33/33	3/4	3/3
Oculogyric crises	86	67/78	33/38	28/33	3/4	3/3
Other neurologic signs						
Sweating	65	51/78	20/38	26/33	2/4	3/3
Developmental retardation	63	49/78	22/38	24/33	1/4	2/3
Dystonia	53	41/78	21/38	16/33	1/4	2/3
Hypertonia	44	35/78	14/38	18/33	1/4	2/3
Feeding/swallowing difficulties	42	33/78	17/38	16/33	0/4	0/3
Dysarthria/speech difficulties	41	32/78	9/38	20/33	1/4	2/3
Hypersalivation	41	32/78	12/38	17/33	1/4	2/3
Ptosis	39	30/78	18/38	10/33	2/4	0/3
Insomnia	37	29/78	11/38	17/33	1/4	0/3
Irritability	35	27/78	12/38	12/33	1/4	2/3
Hypokinesia	32	25/78	8/38	14/33	1/4	2/3
Nasal congestion	31	24/78	10/38	12/33	2/4	0/3
Temperature instability	29	23/78	12/38	9/33	1/4	1/3
Poor head control	28	22/78	10/38	9/33	2/4	1/3
Athetosis	27	20/78	8/38	11/33	0/4	1/3
Poor eye fixation	26	19/78	10/38	9/33	0/4	0/3
Chorea	22	17/78	7/38	9/33	1/4	0/3
Brain imaging						
Abnormal MRI	24	19/78				
Abnormal EEG	13	10/78				
Abnormal CT	6	5/78				

Abbreviation: AADC = aromatic L-amino acid decarboxylase.
[a] For the full list of signs and symptoms and description of radiologic findings, see table e-1 and online information in the JAKE database (http://www.biopku.org).

umented in 86% of patients at the time of investigation. Thus, oculogyric crises and hypotonia can be considered characteristic features of AADC deficiency (table 1). A total of 63% of the patients developed developmental retardation: mental or motor retardation or both. Additional autonomic symptoms such as excessive sweating or temperature instability occurred in 65% and 29% of the patients. Further, most frequent symptoms described were feeding or speech difficulties (42%) and movement disorders like athetosis (27%), chorea (22%), dystonia (53%), or hypokinesia (32%). Poor eye fixation was documented in 19 patients (26%), poor head control in 22 patients (28%), hypersalivation in 32 patients (41%), and hypertonia in 35 patients (44%). A total of 37% of the patients had insomnia and 35% had irritability. In 24 patients (31%), nasal congestion was reported, and in 30 patients (39%), ptosis was evident (table 1).

For more detailed information, see table e-1 or the JAKE database (http://www.biopku.org).

Biochemical investigations. The age at laboratory diagnosis varied from 4 months to 24 years (median 3.9 years). None of the patients was diagnosed in the neonatal period. The results of the CSF, plasma, and urine analyses at the time of diagnosis are shown in table e-2. All patients whose biochemical data are reported showed significantly reduced 5-hydroxyindoleacetic acid (5HIAA), homovanillic acid (HVA), and 3-methoxy-4-hydroxyphenylglycol (MHPG) levels in CSF together with elevations of 5-OH-Trp and 3-*O*-methyldopa (3OMD). In all patients in whom AADC activity in plasma was measured, it was always very low or not detectable. VLA elevation in urine was reported in a few cases and in some elevation was rather mild. L-dopa (3,4-dihydroxyphenylalanine) was, however, normal in 6 out of 78 patients. A typical pattern of CSF metabolites is summarized in figure 2.

Genotypes. We found a wide range of mutations and genotypes (table e-2 and figure e-1), and DNA analysis was available in 49 out of 78 patients. Out of 30 mutations described in the BIOMDB database, 24 different mutations were detected in patients from the JAKE database, of which 8 had not been described earlier (p.L38P, p.Y79C, p.A110Q, p.G123R, p.I42fs, c.876G>A, p.R412W, p.I433fs). In 3 patients (ID#36, ID#37, ID#48), mutations were found on 1 allele only. The substitution mutation in Intron 6, IVS6+4A>T, was by far the most common mutation (allele frequency 45%), followed by p.S250F (allele frequency 10%), p.G102S (allele frequency 8%), and p.R462P (allele frequency 6%). It is conspicuous that all patients with an IVS6+4A>T mutation are of Chinese or Taiwanese origin and 7 patients whose ethnic origin is not known are living in Taiwan. All the other mutations are presented with allele frequency of 1%–3%. The 3 most common genotypes are IVS6+4A>T/IVS6+4A>T (35%), p.S250F/p.S250F (6%), and p.G102S/p.G102S (4%).

Neuroimaging and EEG investigations. A total of 24% of patients showed an abnormal MRI, 13% an abnormal EEG, and 6% an abnormal CT (table 1). The patients with an abnormal EEG mostly showed slow or rapid activity or polyspikes. Patients with abnormal MRI or CT presented with cerebral atrophy, degenerative changes of the white matter, thinning of corpus callosum, prominent ventricular bodies, leukodystrophy-like pattern, or hypomyelination.

Treatment. Although a variety of medications have been used in patients with AADC deficiency, some therapeutic protocols are used more frequently and

Table 2 **Summary of the most frequently used medications in patients with AADC deficiency and recommended treatment modalities**

Medication	Dosage reported in JAKE database	No. of patients	%	Starting dosage,[a] mg/kg/d	Dose per day[a]	Maximal dosage,[a] mg/kg/d
Pyridoxine (B6)[b]	40–1,800 mg/d or 4.0–81 mg/kg/d	55/78	71	50	3	200
Bromocriptine[b]	1.0–45.5 mg/d or 0.013–4.0 mg/kg/d	38/78	49	0.25	3	0.5
Pergolide[b]	0.3–1.5 mg/d or 0.006–0.75 mg/kg/d	12/78	15	0.006	2–3	0.05
Selegiline	0.1–6.0 mg/d or 0.03–1.5 mg/kg/d	19/78	24	0.1	2–3	0.3
Tranylcypromide	1.5–54 mg/d or 0.4–0.5 mg/kg/d	22/78	28	0.1	2	0.5
Trihexyphenidyl	0.231–4.62 mg/d or 0.3–0.5 mg/kg/d	15/78	19	0.1	3	0.5
L-Dopa	400–2,250 mg/d or 11.2–54 mg/kg/d	10/78	13	1	3	15

Abbreviation: AADC = aromatic L-amino acid decarboxylase.
[a] Modified according to Hoffmann and Surtees.[30]
[b] Therapy is usually initiated with a combination of the low-dosage pyridoxine and one of the dopamine agonists (bromocriptine or pergolide). In a second step, monoamine oxidase inhibitor is added (e.g., selegiline). All other medications are added only if the initial treatment protocol fails to improve neurologic symptoms.

pyridoxine is the most common drug used (71% of patients). The dosage reported varied between 40 and 1,800 mg/day (4.0–81 mg/kg/day). Bromocriptine was used in 38 out of 78 patients, with a dosage of 1.0–45.5 mg/day (0.013–4.0 mg/kg/day), and tranylcypromide (1.5–54 mg/day or 0.4–0.5 mg/kg/day) and selegiline (0.03–1.5 mg/kg/day) were applied in 28% and 24% of patients. A total of 19% of patients had a therapeutic trial with trihexyphenidyl with dosages of 0.231–4.62 mg/day (0.3–0.5 mg/kg/day), 15% were tried on pergolide (0.3–1.5 mg/day or 0.006–0.75 mg/kg/day), and 13% of patients were treated with L-dopa (400–2,250 mg/day or 11.2–54 mg/kg/day). The majority of cases showed no or poor response despite different protocols and a combination of different drugs. Only 15 patients (nos. 10, 13, 14, 15, 26, 27, 45, 47, 53, 55, 56, 64, 66, 67, and 71) were reported with good or very good clinical benefit (improvement in at least 5 symptoms). Patients 1–3 have been previously described with favorable clinical benefit,[6] and 2 other patients (26 and 27) with an excellent response to MAO inhibitor and dopamine agonist therapy.[20] There was no significant difference between 2 groups (responder and nonresponder) with regard to biochemical and genetic data.

A total of 73 patients (96%) were clinically inconspicuous before the age of 10 years and most of them

Figure 2 **CSF metabolites**

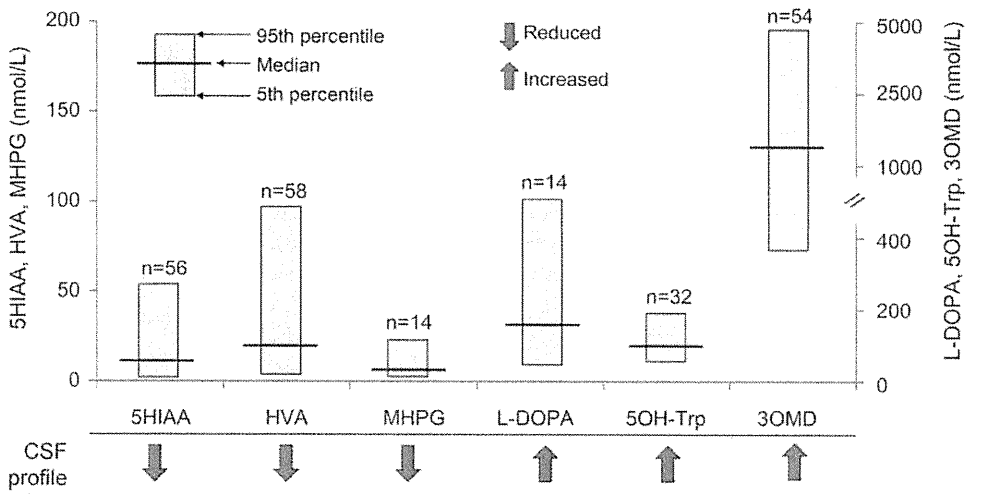

CSF concentrations (median and 5th–95th percentile) of key neurotransmitter metabolites in patients with aromatic L-amino acid decarboxylase deficiency at the time of diagnosis. 3OMD = 3-O-methyldopa; 5HIAA = 5-hydroxyindoleacetic acid; 5OH-Trp = 5-hydroxytryptophan; HVA = homovanillic acid; L-dopa = 3,4-dihydroxyphenylalanine; MHPG = 3-methoxy-4-hydroxyphenylglycol. For reference ranges, see table e-2. These may differ between laboratories.

were started on medication immediately after diagnosis. Many of these patients also developed additional non-neurologic symptoms such as ptosis, excessive sweating, temperature instability, and nasal congestion (table 1).

DISCUSSION In this study, we documented clinical, biochemical, and molecular data of 78 patients with AADC deficiency, tabulated in the JAKE database of pediatric neurotransmitter disorders. A total of 32 cases have not been published previously. The clinical presentation of these new patients is in line with the clinical picture of AADC deficiency described in the literature.[2,5,6,18,24,25] The most frequent neurologic signs and symptoms were muscular hypotonia and oculogyric crises and approximately half of the patients showed movement disorders with hypokinesia, dystonia, athetosis, and chorea. While hypotonia is a rather nonspecific feature, oculogyric crises are typical for AADC-deficient patients and were not present or not reported at the age of investigation in only 11 patients.[14,25,26] Seven previously unreported cases (49, 52, 53, 60, 61, 63, and 74) also did not present with oculogyric crises at the age of investigation (5 months–11.5 years); however, it is possible that some of these patients will develop such episodes in the future, particularly since some of them were not on treatment. A total of 49 patients were reported with mental or motor retardation.

In general, most of the signs and symptoms described in patients with AADC deficiency can be assigned to deficiencies of dopamine, norepinephrine, epinephrine, and serotonin. Dopamine is synthesized in substantia nigra, ventral tegmentum, and hypothalamus, and its deficiency affects voluntary movements, cognitive function, and emotion, but also hormonal-related functions. Norepinephrine and epinephrine deficiency affects attention, mood, sleep, cognition, and stress hormones, and disturbance in serotonin biosynthesis affects appetite, sleep, memory, learning, body temperature, mood, cardiovascular function, and endocrine functions. Consequently, AADC-deficient patients present with parkinsonism and dystonia, motor activity, and sleep problems (dopamine functions); autonomic dysfunction, temperature instability, and ptosis (norepinephrine and epinephrine function); and sleep disorders, memory and learning disability, and behavioral disturbance (serotonin functions).[27]

Brain imaging and EEG revealed normal findings in most patients. Ten patients had an abnormal EEG, mostly showing slow or rapid activity or polyspikes.[4,14,18,19,28] Five patients with an abnormal brain CT and 19 patients with an abnormal MRI presented with cerebral atrophy, degenerative changes of the white matter, thinning of corpus callosum, prominent ventricular bodies, leukodystrophy-like pattern, hypomyelination, or adult pattern of myelination.[2,14,19,22,25,28,29]

The clinical phenotype, although quite typical in classic patients, will hardly ever be recognized as AADC deficiency due to its rarity, physicians thus being unfamiliar with the disorder. In general, the results of biochemical investigations will point to AADC deficiency as the underlying cause in a child with a complex neurologic disorder. Laboratory protocol for the diagnosis of AADC deficiency includes investigation of metabolites of dopamine and serotonin (HVA, MHPG, L-dopa, 3OMD, 5-OH-Trp, and 5HIAA) in CSF,[8] AADC activity in plasma,[3] and organic acids (VLA) in urine.[19] Although measurement of VLA within the organic acids profile would be the most practical approach in the diagnosis of AADC deficiency, a number of patients who we investigated presented with only mildly elevated concentrations of urinary VLA (data not shown). Measurement of additional metabolites in urine such as vanilpyruvic acid and N-acetyl-vanilalanine, both metabolites of VLA, may increase the sensitivity of this approach.[19] Thus, CSF investigation of neurotransmitter metabolites is essential for the diagnosis. As shown in table e-2 and figure 2, all patients whose biochemical data are known presented with a typical pattern of metabolites in CSF, specifically reduced concentrations of HVA, 5HIAA, and MHPG, and an elevation of 3OMD, L-dopa, and 5-OH-Trp. L-dopa was reported as elevated in 40 out of 78 patients. In 32 patients, it was not measured (nos. 1, 9, 11, 12, 14, 16–20, 26–35, 48, 49, 58–63, 70, and 75–78), and in patients 13, 53, 69, and 71–73, it was normal. Some variability in the biochemical data could, however, relate to diurnal variation. If there is diurnal variation, then any correlation between treatment response and biochemical data could be obscured by this variation.

In 49 patients, mutation analysis of the *DDC* gene was performed. Different point mutations were identified; 8 mutations have not previously been reported in AADC-deficient patients (p.L38P, p.Y79C, p.A110Q, p.G123R, p.I42fs, c.876G>A, p.R412W, p.I433fs). With the exception of patients with Chinese origin with a common splice mutation IVS6+4A>T, most patients harbor private mutations spread out through the entire *DDC* gene (table e-2). There is no indication for a genotype–phenotype correlation.

The therapy is aimed at correcting the neurotransmitter abnormalities, especially those of serotonin and catecholamines. Unfortunately, a substitution therapy with neurotransmitter precursors L-dopa and 5-

hydroxytryptophan is not effective in nearly all AADC-deficient patients, as they cannot be further metabolized and in fact already circulate in enormous amounts. Nevertheless, 3 siblings responded dramatically to L-dopa. They carry a homozygous mutation affecting the binding of the substrate L-dopa to the enzyme.[5] Thus, treatment strategies are aiming either at an augmentation of residual AADC activity with pyridoxine and PLP or the use of MAO-B inhibitors and dopamine agonists are commonly used.

Patients received dopamine receptor agonists, anticholinergics, monoaminoxidase inhibitors, α-adrenergic agonists, selective serotonin reuptake inhibitors, cofactor of AADC (pyridoxine or PLP), catechol-*O*-methyltransferase inhibitors, precursors of dopamine and serotonin (L-dopa, 5-OH-Trp), L-dopa decarboxylase inhibitors, folinic acid, and melatonin. Other medications were used to lesser degree. The overall response to drug therapy was good in 15 patients, with unsatisfactory or no response in the other 63 patients. There may be a difference in response to treatment between male and female patients, as reported by Pons et al.[6] Ten out of the 15 patients with a satisfactory clinical benefit were male. However, more male than female patients were investigated. There were 41 male patients, 31 female patients, and 6 patients with unknown sex who took part in our study. The 15 patients with a good clinical response still have different symptoms that never completely resolved.

First-choice medications appear to be dopamine agonists such as bromocriptine or pergolide in combination with pyridoxine, and MAO inhibitors such as selegiline in the second step (table 2). Bromocriptine is usually given at a starting dosage of 0.25 mg/kg/day divided in 3 doses per day. Another dopamine agonist, pergolide, should be given at a very low starting dosage of 0.006 mg/kg/day twice a day. Beneficial effect of pergolide was described in patients with a severe neurotransmitter deficiency due to tetrahydrobiopterin deficiency. Alternatively to selegiline, tranylcypromine can be given in 1–3 doses a day at a dosage around 8 mg/day. The therapy with trihexyphenidyl should start at a dosage of 1–2 mg/kg 3 times daily. The dosage should then be increased by 1 or 2 mg/day each week until the child shows any improvement, the child develops side effects, or a limit of 10 mg/kg/day is reached. As alternative therapy, L-dopa may be given. L-dopa should be given 3 times a day at a dosage of ≤15 mg/kg/day. L-dopa should be increased in steps of not more than 1 mg/kg over days, weeks, or sometimes several months. It should be introduced slowly because of receptor hypersensitivity in early-diagnosed severe cases, and start at very low doses given up to 6 times a day. In late-diagnosed severe cases, patients maximally tolerate a dose of up to 10 mg/kg/day, which should be given for 6 months before deciding whether it is beneficial or not. Additional carbidopa treatment should be avoided, because of a possible deterioration of symptoms. Pyridoxine, precursor of the natural cofactor of AADC, should not be given at doses of >200 mg/kg/day.[30] Pyridoxine is first phosphorylated to pyridoxine 5′-phosphate and subsequently converted to PLP. There is evidence that an optimal level of PLP is important for AADC stability and that PLP may be required for the maintenance of AADC activity.[13]

Folinic acid substitution in AADC-deficient patients is recommended at a dosage of 10–20 mg/day because of possible cerebral folate depletion due to methylation of accumulated L-dopa.

Drug therapy in patients with AADC deficiency is a challenge and unfortunately there are still no good therapeutic strategies available. For many patients, the overall outcome is disappointing.

There is a new hope that AADC-deficient patients may benefit from gene therapy in the future. By delivering the human *DCC* gene into patients' cells,[13] this technique may stabilize expression of a functional AADC protein. Similar attempts are in progress for patients with Parkinson disease.[31] In a phase I safety trial, patients with moderate to advanced Parkinson disease received bilateral infusion of a low dose of the adeno-associated viral hAADC vector into the putamen. This gene therapy approach has been well-tolerated and shows evidence of sustained gene expression.

AUTHOR AFFILIATIONS

From the Division of Clinical Chemistry and Biochemistry (L.B., N.B.), University Children's Hospital, Zürich; Zürich Center for Integrative Human Physiology (ZIHP) (N.B.), Zürich, Switzerland; Genetic Department (L.H.N., W.T.K., G.S.C.), Kuala Lumpur Hospital, Jalan Pahang, Kuala Lumpur; Prince Court Medical Centre (Y.S.C.), Kuala Lumpur, Malaysia; Department of Pediatrics (W.L.H., W.T.L.), National Taiwan University Hospital, Taipei, Taiwan; Department of Pediatric Neurology (M.A.A.P.W.), Donders Centre for Brain, Cognition and Behaviour (M.M.V.), Departments of Neurology and Laboratory Medicine (M.M.V., T.W.), Radboud University Nijmegen Medical Centre, Nijmegen, the Netherlands; Pediatrics-Metabolic Center (L.R.), University Hospital Leuven, Leuven, Belgium; Department of Child Neurology and Psychiatry (S.O., D.T.), IRCCS C. Mondino Institute of Neurology Foundation, Pavia; Department of Child Neurology and Psychiatry (P.A.), Spedali Civici, Brescia, Italy; Centre Hospitalier Intercommunal Annemasse (H.T.), Service de Pédiatrie et de Néonatalogie, Annemasse, France; Division of Metabolic Disorders (J.E.A.), CHOC Children's, Orange, CA; Division of Pediatric Neurology and Developmental Pediatrics (S.T.), Department of Pediatrics, National University of Singapore and National University Hospital, Singapore; Department of Molecular Neurosciences (G.F.A., S.H.), UCL Institute of Neurology, London, UK; Pediatric Metabolism (I.K.), University Children's Hospital, Geneva, Switzerland; Department of Pediatrics (M.K.), Yamagata University Hospital, Yamagata, Japan; Division of Metabolic Disorders (A.B.), Department of Pediatrics, University Hospital, Padua, Italy; and Zentrum für Kinder- und Jugendmedizin der Universität Heidelberg (C.M., G.F.H.), Heidelberg, Germany.

ACKNOWLEDGMENT

The authors thank Professor Felix Sennhauser, Medical Director of the University Children's Hospital in Zürich, for continuous support.

DISCLOSURE

L. Brun reports no disclosures. Dr. Ngu received a speaker honorarium from Genzyme Corporation. Dr. Keng, Dr. Ch'ng, Dr. Choy, Dr. Hwu, Dr. Lee, and Dr. Willemsen report no disclosures. Dr. Verbeek serves as a consultant for Schering-Plough Corp. and receives research support from Schering-Plough Corp., the AADC Research Trust, Internationale Stichting Alzheimer Onderzoek, Zon-MW, and the Center for Translational Molecular Medicine. Dr. Wassenberg reports no disclosures. Dr. Régal has received funding for travel and speaker honoraria from Genzyme Corporation. Dr. Orcesi, Dr. Tonduti, and Dr. Accorsi report no disclosures. Dr. Testard serves on a scientific advisory board for the French Neurology Paediatric Association and has received funding for travel from Sandoz, Endo Pharmaceuticals, and UCB. Dr. Abdenur has received research support from the Hailey's Wish Foundation. Dr. Tay receives research support from the National Medical Research Council, Singapore, and the Biomedical Research Council, Singapore. G.F. Allen reports no disclosures. Dr. Heales received a speaker honorarium from Merck Serono. Dr. Kern has received research support from Ligue Genevoise Contre le Cancer. Dr. Kato has received research support from Grant-in-Aid for Scientific Research from the Japan Society for the Promotion of Science, the Ministry of Health, Labor and Welfare of Japan, and from the Japan Epilepsy Research Foundation. Dr. Burlina and Dr. Manegold report no disclosures. Dr. Hoffmann serves as Editor-in-Chief of the *Journal of Inherited Metabolic Diseases* and *Neuropediatrics* and on editorial advisory boards for *Monatsschrift Kinderheilkunde*, *The Open Pediatric Medicine Journal*, the *World Journal of Pediatrics*, and *Kinderneurologie in Klinik und Praxis*; and receives royalties for the publication of *Pediatric Endocrinology and Inborn Errors of Metabolism* (The McGraw-Hill Companies Medical, 2009) and *Core Handbook in Pediatrics: Inherited Metabolic Diseases* (Lippincott Williams & Wilkins, 2002). Dr. Blau has served on a scientific advisory board for Merck Serono; has received funding for travel from Merck Serono and BioMarin Pharmaceutical Inc.; and has served on the editorial board of *Molecular Genetics and Metabolism* and as Communicating Editor for the *Journal of Inherited Metabolic Diseases*.

Received October 23, 2009. Accepted in final form February 8, 2010.

REFERENCES

1. Hyland K, Clayton PT. Aromatic amino acid decarboxylase deficiency in twins. J Inherit Metab Dis 1990;13:301–304.
2. Hyland K, Surtees RA, Rodeck C, Clayton PT. Aromatic L-amino acid decarboxylase deficiency: clinical features, diagnosis, and treatment of a new inborn error of neurotransmitter amine synthesis. Neurology 1992; 42:1980–1988.
3. Verbeek MM, Geurtz PBH, Willemsen MAAP, Wevers RA. Aromatic L-amino acid decarboxylase enzyme activity in deficient patients and heterozygotes. Mol Genet Metab 2007;90:363–369.
4. Swoboda KJ, Hyland K, Goldstein DS, et al. Clinical and therapeutic observations in aromatic L-amino acid decarboxylase deficiency. Neurology 1999;53:1205–1211.
5. Chang YT, Sharma R, Marsh JL, et al. Levodopa-responsive aromatic L-amino acid decarboxylase deficiency. Ann Neurol 2004;55:435–438.
6. Pons R, Ford B, Chiriboga CA, et al. Aromatic L-amino acid decarboxylase deficiency: clinical features, treatment, and prognosis. Neurology 2004;62:1058–1065.
7. Lovenberg W, Weissbach H, Udenfriend S. Aromatic amino acid decarboxylase. J Biol Chem 1962;237:89–93.
8. Hyland K, Clayton P. Aromatic L-amino acid decarboxylase deficiency: diagnostic methodology. Clin Chem 1992; 38:2405–2410.
9. Hyland K, Biaggioni I, Elpelg ON, Nyggard TG, Gibson KM. Disorders of neurotransmitter metabolism. In: Blau N, Duran M, Blaskovics M, eds. Physician's Guide to the Laboratory Diagnosis of Metabolic Diseases. London: Chapman & Hall; 1996: 79–98.
10. Heales SRH. Biogenic amines. In: Blau N, Duran M, Gibson KM, eds. Laboratory Guide to the Methods in Biochemical Genetics. Berlin: Springer-Verlag; 2008: 703–715.
11. Maller A, Hyland K, Milstien S, Biaggioni I, Butler IJ. Aromatic L-amino acid decarboxylase deficiency: clinical features, diagnosis, and treatment of a second family. J Child Neurol 1997;12:349–354.
12. Haavik J, Blau N, Thony B. Mutations in human monoamine-related neurotransmitter pathway genes. Hum Mutat 2008;29:891–902.
13. Allen GF, Land JM, Heales SJ. A new perspective on the treatment of aromatic l-amino acid decarboxylase deficiency. Mol Genet Metab 2009;97:6–14.
14. Billette de Villemeur T, de Lonlay P, Poggi-Travert F, et al. Monoamine decarboxylase deficiency. Arch Pediatr 1996;3 suppl 1:167s–168s.
15. Abeling NG, van Gennip AH, van Cruchten A, Westra M, Wijburg FA, Barth PG. Aromatic-L-amino acid decarboxylase deficiency: a new case with a mild clinical presentation and unexpected laboratory findings. J Inherit Metab Dis 1997;20:100.
16. Korenke CG, Christen HJ, Hyland K, Hunneman DH, Hanefeld F. Aromatic L-amino acid decarboxylase deficiency: an extrapyramidal movement disorder with oculogyric crises. Eur J Pediatr Neurol 1997;2/3:67–71.
17. Brautigam C, Wevers RA, Hyland K, Sharma RK, Knust A, Hoffman GF. The influence of L-dopa on methylation capacity in aromatic L-amino acid decarboxylase deficiency: biochemical findings in two patients. J Inherit Metab Dis 2000;23:321–324.
18. Fiumara A, Brautigam C, Hyland K, et al. Aromatic L-amino acid decarboxylase deficiency with hyperdopaminuria: clinical and laboratory findings in response to different therapies. Neuropediatrics 2002;33:203–208.
19. Abdenur JE, Abeling N, Specola N, et al. Aromatic L-aminoacid decarboxylase deficiency: unusual neonatal presentation and additional findings in organic acid analysis. Mol Genet Metab 2006;87:48–53.
20. Tay SK, Poh KS, Hyland K, et al. Unusually mild phenotype of AADC deficiency in 2 siblings. Mol Genet Metab 2007;91:374–378.
21. Lee HF, Tsai CR, Chi CS, Chang TM, Lee HJ. Aromatic L-amino acid decarboxylase deficiency in Taiwan. Eur J Paediatr Neurol 2009;13:135–140.
22. Ide S, Sasaki M, Kato M, et al. Abnormal glucose metabolism in aromatic l-amino acid decarboxylase deficiency. Brain Dev Epub 2009 Jun 9.
23. Blau N, Duran M, Gibson KM. Laboratory Guide to the Methods in Biochemical Genetics. Berlin: Springer-Verlag; 2008.
24. Swoboda KJ, Saul JP, McKenna CE, Speller NB, Hyland K. Aromatic L-amino acid decarboxylase deficiency: overview of clinical features and outcomes. Ann Neurol 2003;54 suppl 6:S49–S55.

25. Manegold C, Hoffmann GF, Degen I, et al. Aromatic L-amino acid decarboxylase deficiency: clinical features, drug therapy and follow-up. J Inherit Metab Dis 2009;32:371–380.
26. Burlina AB, Burlina AP, Hyland K, Bonafé L, Blau N. Autistic syndrome and aromatic L-amino acid decarboxylase deficiency. J Inherit Metab Dis 2001;24:34.
27. Siegel GJ, Agranoff BW, Albers RW, Fisher SK, Uhler MD. Basic Neurochemistry: Molecular, Cellular, and Medical Aspects. Philadelphia: Lippincott Williams & Wilkins; 1999.
28. Ito S, Nakayama T, Ide S, et al. Aromatic l-amino acid decarboxylase deficiency associated with epilepsy mimicking non-epileptic involuntary movements. Dev Med Child Neurol 2008;50:1–3.
29. Anselm IA, Darras BT. Catecholamine toxicity in aromatic L-amino acid decarboxylase deficiency. Pediatr Neurol 2006;35:142–144.
30. Hoffmann GF, Surtees R. Disorders of neurotransmission. In: Blau N, Hoffmann G, Leonard J, Clarke J, eds. Physician's Guide to the Treatment and Follow-up of Metabolic Diseases. Heidelberg: Springer; 2006: 35–42.
31. Eberling JL, Jagust WJ, Christine CW, et al. Results from a phase I safety trial of hAADC gene therapy for Parkinson disease. Neurology 2008;70:1980–1983.

ELSEVIER

Brain & Development 32 (2010) 506–510

BRAIN & DEVELOPMENT
Official Journal of the Japanese Society of Child Neurology

www.elsevier.com/locate/braindev

Case report

Abnormal glucose metabolism in aromatic L-amino acid decarboxylase deficiency

Shuhei Ide [a,b], Masayuki Sasaki [a,*], Mitsuhiro Kato [c], Takashi Shiihara [c,d], Satoru Kinoshita [a], Jun-ya Takahashi [a], Yu-ichi Goto [b]

[a] *Department of Child Neurology, National Center of Neurology and Psychiatry (NCNP), 4-1-1 Ogawahigashi-cho, Kodaira, Tokyo 187-8551, Japan*
[b] *Department of Mental Deficiency, National Institute of Neuroscience, NCNP, Kodaira, Tokyo 187-8553, Japan*
[c] *Department of Pediatrics, Yamagata University Hospital, Yamagata, Japan*
[d] *Department of Neurology, Gunma Children's Medical Center, Shibukawa, Gunma, Japan*

Received 7 February 2009; received in revised form 29 April 2009; accepted 10 May 2009

Abstract

We report sibling cases of aromatic L-amino acid decarboxylase (AADC) deficiency, which is a very rare congenital metabolic disorder. These patients were born to healthy and non-consanguineous parents, and presented oculogyric crises, paroxysmal dystonic attacks, and severe psychomotor retardation since early infancy. In cerebrospinal fluid the levels of homovanilic acid and 5-hydroxyindoleacetic acid were very low and the level of L-dopa was very high. The diagnosis was confirmed by the lack of AADC activity in plasma, and a point mutation in the *AADC* gene. MRI revealed a slightly small volume of the prefrontal areas and normal myelination in both patients. Positron emission tomography using 2-deoxy-2[^{18}F] fluoro-D-glucose was performed in one patient, which revealed hypometabolism in the prefrontal cortex and bilateral basal ganglia with a little laterality. These findings suggested that the severe dystonic features were caused by abnormal function of bilateral basal ganglia and severe psychomotor retardation could be due to abnormalities in prefrontal cortical activity.

Keywords: AADC deficiency; MRI; PET; Prefrontal cortex; Caudate nucleus

1. Introduction

Aromatic L-amino acid decarboxylase (AADC or dopa decarboxylase; DDC) deficiency (OMIM #608643) is an extremely rare congenital metabolic disorder and one of the infantile movement disorders, which is very intractable to treat [1–4]. Although less than 100 cases have been reported worldwide [1–8], a relatively high occurrence rate was reported in Taiwan [7]. AADC converts L-dopa to dopamine and 5-hydroxy tryptophan to serotonin, and its deficiency results in the depletion of both dopamine and serotonin in the brain. As a consequence, several characteristic symptoms are caused.

We experienced sibling cases of AADC deficiency, confirmed by enzymatic and genetic analysis. We report magnetic resonance imaging (MRI) findings in both cases, and positron emission tomography (PET) using 2-deoxy-2[^{18}F] fluoro-D-glucose (FDG) between dystonic attacks was performed in patient 1.

2. Case reports

2.1. Patient 1

This 3-year-old boy was born to healthy and unrelated parents with mild asphyxia at full term. He cried

* Corresponding author. Tel.: +81 42 341 2711; fax: +81 42 344 6745.
E-mail address: masasaki@ncnp.go.jp (M. Sasaki).

0387-7604/$ - see front matter © 2009 Elsevier B.V. All rights reserved.
doi:10.1016/j.braindev.2009.05.004

Table 1
The concentration of catecholamine of the CSF.

	L-Dopa	HVA	MHPG	5-HIAA
Patient 1	13.6	5.7	<1.0	<1.0
Patient 2	27.4	12.2	<1.0	<1.0
Normal range	<2.0(ng/ml)	28–200(ng/ml)	6.5–51(ng/ml)	17–116(ng/ml)

HVA, homovanillic acid; MHPG, 3-methoxy-4-hydroxy-phenylglycol; 5HIAA, 5-hydroxyindoleacetic acid.

weakly, was motion-less since birth, and needed tube feeding for 1 week. He first showed oculogyric crisis at 3 months of age, and had similar attacks several times a week. Oculogyric crisis usually lasted about 30 min. He also suffered from generalized dystonic attacks for 30–120 min several times a week. Opisthotonus or bicycle-riding movements were observed during these attacks. He showed visual pursuit at 6 months of age, but had not yet obtained head control or rolling over. He had a severe intellectual and motor developmental delay. He was always nasally congested and his face was frequently running with sweat during wakefulness.

A neurological examination between dystonic attacks revealed general hypotonia, paucity of movement, slightly exaggerated deep tendon reflexes and pathological reflexes. Eye movement was normal. Ordinary blood analyses were normal. An electroencephalogram (EEG) showed no paroxysmal discharges during either dystonic attacks or inter-

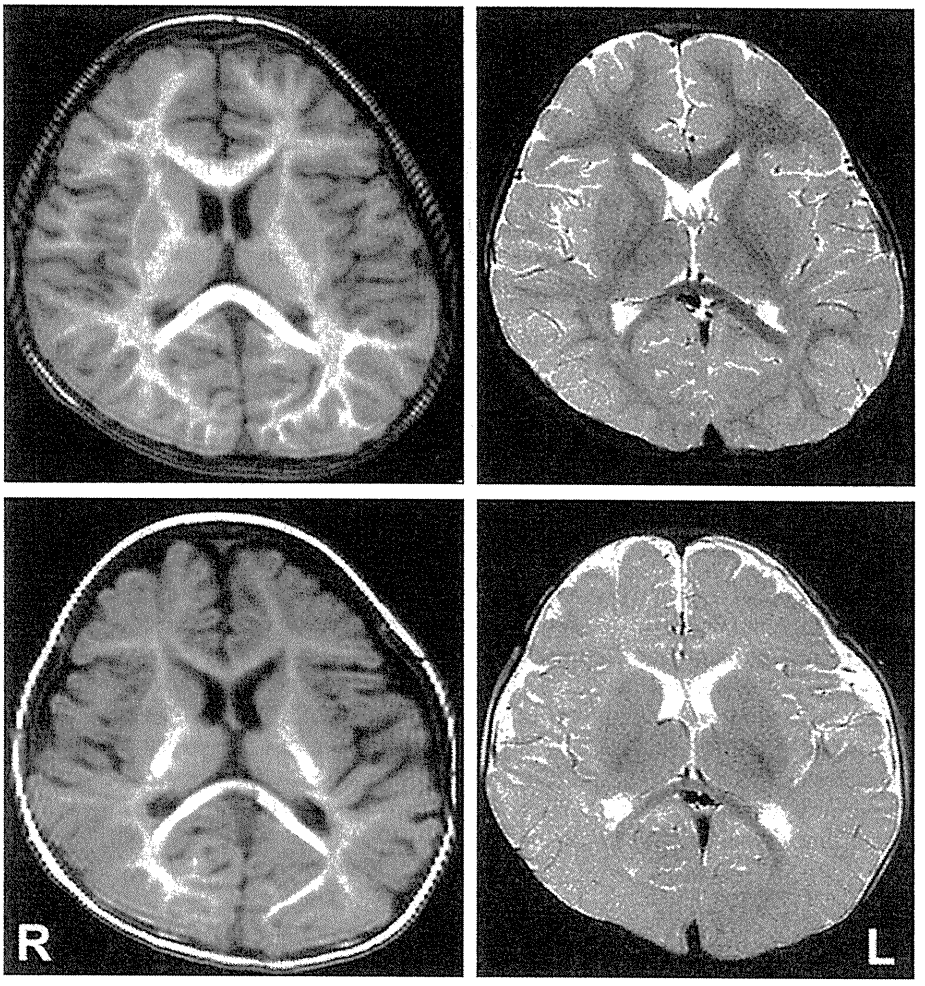

Fig. 1. Axial T1-weighted (left) and T2-weighted (right) MRI at the level of the putamen. Upper row is patient 1 and lower row is patient 2. MRI shows a slightly small volume of the prefrontal areas in both patients. The volumes of basal ganglia and brain cortex are normal, and myelination is also normal. No abnormal intensity areas are seen.

mittent states. A catecholamine analysis of the cerebrospinal fluid (CSF) revealed a very high concentration of L-dopa and a very low concentration of homovanilic acid (HVA) and 5-hydroxyindoleacetic acid (5-HIAA) (Table 1). These results strongly suggested AADC deficiency.

2.2. Patient 2

This 6-month-old girl was the younger sister of patient 1. She was born healthy with no adverse events. She also showed oculogyric crisis since 1 month of age, and paroxysmal general hypertonia lasting for a few hours since 3 months of age but she was alert during the attack. She had not yet obtained head control or rolling over. She also disclosed general hypotonia and paucity of movement between hypertonic attacks. Her CSF revealed a high concentration of L-dopa and a very low concentration of HVA and 5-HIAA (Table 1).

2.3. AADC activity

AADC activity was measured in the serum to confirm the diagnosis using previously reported methods [9]. Serum AADC activity was very low in both patients (AADC activity: 0.5 pmol/min/ml in patient 1, 0.4 pmol/min/ml in patient 2; normal; 50–100).

2.4. Gene analysis

The *AADC* gene mutation was analyzed after obtaining informed consent from the parents of the patients. Genomic DNA from peripheral blood of the patients was extracted according to standard procedures. Each exon of the *AADC* gene was amplified by PCR using primers designed to amplify the coding and flanking non-coding *AADC* regions. Bidirectional cycle sequencing reactions were performed with the ABI Big Dye Terminator Sequencing Kit (Applied Biosystems: Foster city, CA, USA), and the purified products were subject to an automated capillary array sequencer (ABI 3100, Applied Biosystems). Sequencing results revealed a heterozygous point mutation (g.329C > A). The other mutation was not detected. We confirmed that this point mutation was not present in 50 normal Japanese controls.

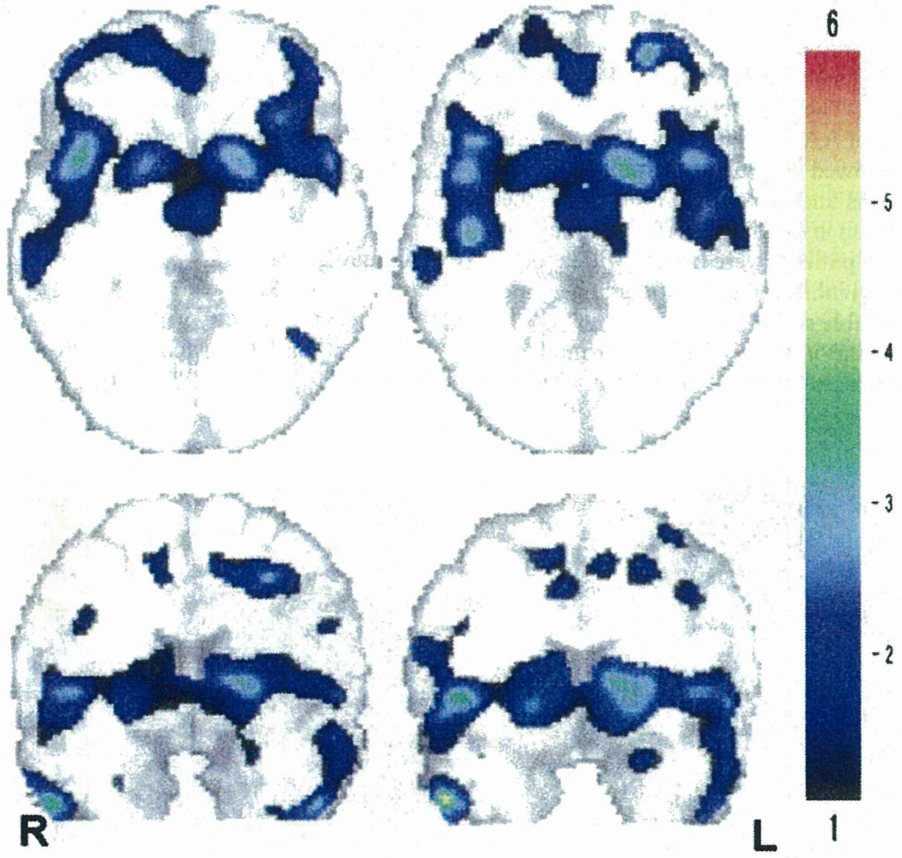

Fig. 2. Easy Z-score imaging (eZIS) analysis of FDG-PET in patient 1. Hypometabolim is observed in bilalateral caudate nuculei to putamina (lower in the left side) and insular cortex with some laterality. Upper; axial section, lower; coronal section.

3. Neuroradiological studies

MRI: Brain MRI in both patients revealed a slightly small volume of the prefrontal areas (Fig. 1) and normal myelination. No abnormal findings in the basal ganglia were observed.

PET: Glucose metabolism was evaluated by FDG-PET in patient 1. We evaluated the results by using an easy Z-score imaging system (eZIS) [10], eZIS revealed hypometabolism in both caudate nuclei and putamina with some laterality (lower in the left side) (Fig. 2) and prefrontal cortex (Fig. 3). The area in which the level of the area was lower than −2SD compared with the standard is colored with purple or blue and the area lower than −3SD is colored with green.

4. Discussion

Patient 1 was at first assumed to have cerebral palsy (CP) because he was born with mild asphyxia. He had been diagnosed with a dystonic type of CP before patient 2 was born. Patient 2, who was born healthy, showed oculogyric crises and dystonic attacks. Since these symptoms were the same as those in patient 1, it was presumed that they both had a basic disorder. Repeated attacks of dystonia reminded us of childhood movement disorders, especially neurotransmitter diseases, and the catecholamine in the CSF indicated an abnormality in the level of neurotransmitters. The low activity of AADC confirmed the diagnosis of AADC deficiency. The gene analysis of the *AADC* showed heterozygous mutation. Since we examined all exons and intron–exon junctions, there must be other mutation in other area. After the diagnosis was established, both patients were treated with a monoamine oxidase (MAO) inhibitor and a dopamine agonist, but showed no favorable response.

In MRI studies, the volume of the prefrontal area was reduced in both cases by visual inspection, although we did not performed volumetric study. The volume of the basal ganglia was normal.

We performed FDG-PET in patient 1 to investigate the brain glucose metabolism. The eZIS analysis revealed hypometabolism in both basal ganglia and prefrontal cortex. To our knowledge, these findings have not yet been reported in other patients with AADC deficiency [3].

In AADC deficiency, both dopamine and serotonin depletion must have occurred in the brain. Dopamine is mostly involved in substantia nigra and basal ganglia circuits. Hypometabolism in caudate nuclei shown in this FDG-PET study probably could be the cause the symptoms of dystonia and muscle tone abnormality.

The mechanism for the slightly small size and hypometabolism in the prefrontal cortex was not identified. Mesencephalic dopaminergic neurons are known to project to the prefrontal cortex and striatum [11]. The dopamine depletion probably causes dysfunction in dopaminergic innervation, and depleted dopaminergic pathways in the prefrontal cortex probably cause the occurrence of prefrontal cortical dysfunction. Similar dysfunction could occur in the serotonergic pathways. Most patients with AADC deficiency have both severe motor developmental and severe intellectual disability, which might be explained by the prefrontal cortical dysfunction.

Both dopamine and serotonin depletion could produce not only basal ganglia dysfunction but also prefrontal cortical dysfunction, especially in the developing brain.

Acknowledgments

The authors are very grateful to Hiroshi Matsuda M.D. at Saitama Medical Center for providing eZIS analysis for FDG-PET study.

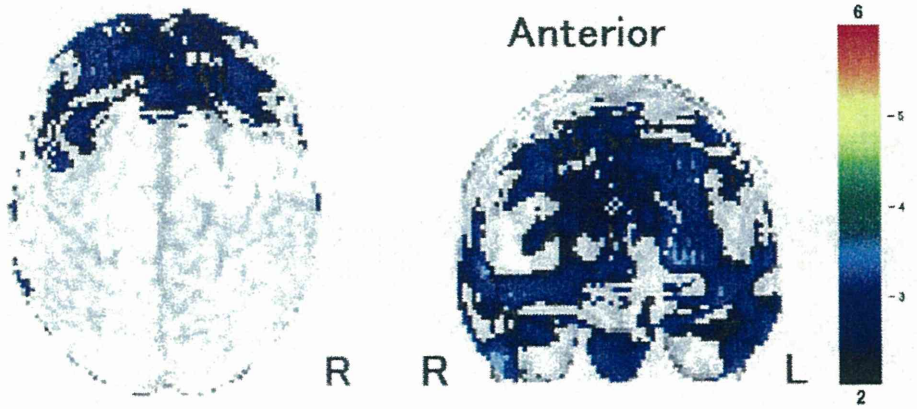

Fig. 3. eZIS analysis of FDG-PET in the projected view show hypometabolism in the prefrontal cortex. Left: from the upper side. Right: from the anterior side.

This study was supported in part by the Research Grant (20B-14) for Nervous and Mental Disorders from the Ministry of Health, Labor and Welfare.

References

[1] Hyland K, Surtees RA, Rodeck C, Clayton PT. Aromatic L-amino acid decarboxylase deficiency: clinical features, diagnosis, and treatment of a new inborn error of neurotransmitter amine synthesis. Neurology 1992;42:1980–8.

[2] Swoboda KJ, Hyland K, Goldstein DS, Kuban KC, Arnold LA, Holmes CS, et al. Clinical and therapeutic observations in aromatic L-amino acid decarboxylase deficiency. Neurology 1999;53:1205–11.

[3] Swoboda KJ, Saul JP, McKenna CE, Speller NB, Hyland K. Aromatic L-amino acid decarboxylase deficiency: overview of clinical features and outcomes. Ann Neurol 2003;54(Suppl 6): S49–55.

[4] Pons R, Ford B, Chiriboga CA, Clayton PT, Hinton V, Hyland K, et al. Aromatic L-amino acid decarboxylase deficiency: clinical features, treatment, and prognosis. Neurology 2004;62:1058–65.

[5] Maller A, Hyland K, Milstien S, Biaggioni I, Butler IJ. Aromatic L-amino acid decarboxylase deficiency: clinical features, diagnosis, and treatment of a second family. J Child Neurol 1997;12: 349–54.

[6] Korenke GC, Christen HJ, Hyland K, Hunneman DH, Hanefeld F. Aromatic L-amino acid decarboxylase deficiency: an extrapyramidal movement disorder with oculogyric crises. Eur J Paediatr Neurol 1997;1:67–71.

[7] Lee HF, Tsai CR, Chi CS, Chang TM, Lee HJ. Aromatic L-amino acid decarboxylase deficiency in Taiwan. Eur J Paediatr Neurol 2008;591:88–95.

[8] Ito S, Nakayama T, Ide S, Ito Y, Oguni H, Goto YI, et al. Aromatic L-amino acid decarboxylase deficiency associated with epilepsy mimicking non-epileptic involuntary movement. Dev Med Child Neurol 2008;50:876–8.

[9] Hyland K, Clayton PT. Aromatic L-amino acid decarboxylase deficiency: diagnostic methodology. Clin Chem 1992;38: 2405–10.

[10] Minoshima S, Frey KA, Koeppe RA, Foster NL, Kuhl ED. A diagnostic approach in Alzheimer's disease using three-dimensional stereo tactic surface projections of fluoro-18-FDG PET. J Nucl Med 1995;36:1238–48.

[11] Franke H, Shelhorn N, Illes P. Dopaminergic neurons develop axonal projections to their target areas in organotypic co-cultures of the ventral mesencephalon and the striatum/prefrontal cortex. Neurochem Int 2003;42:431–9.

Epilepsy Research (2010) 88, 100–107

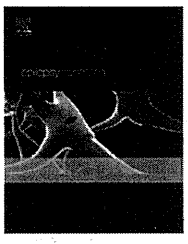

journal homepage: www.elsevier.com/locate/epilepsyres

MEG time–frequency analyses for pre- and post-surgical evaluation of patients with epileptic rhythmic fast activity

Keitaro Sueda[a], Fumiya Takeuchi[b], Hideaki Shiraishi[a], Shingo Nakane[c], Naoko Asahina[a], Shinobu Kohsaka[a], Hideyuki Nakama[d], Taisuke Otsuki[d], Yutaka Sawamura[e], Shinji Saitoh[a,*]

[a] *Department of Pediatrics, Hokkaido University Graduate School of Medicine, North 15 West 7, Kita-ku, Sapporo, 060-8638, Japan*
[b] *Department of Health Science, Hokkaido University School of Medicine, Japan*
[c] *Division of Magnetoencephalography, Hokkaido University Hospital, Japan*
[d] *Department of Neurosurgery, Musashi Hospital, National Center of Neurology and Psychiatry, Japan*
[e] *Department of Neurosurgery, Hokkaido University Graduate School of Medicine, Japan*

Received 4 April 2009; received in revised form 21 September 2009; accepted 4 October 2009
Available online 6 November 2009

KEYWORDS
Magnetoencephalography;
Fast activity;
Fourier transform;
Time–frequency analysis;
Symptomatic localization-related epilepsy;
Surgical evaluation

Summary
Purpose: To evaluate the effectiveness of surgery for epilepsy, we analyzed rhythmic fast activity by magnetoencephalography (MEG) before and after surgery using time–frequency analysis. To assess reliability, the results obtained by pre-surgical MEG and intraoperative electrocorticography were compared.
Methods: Four children with symptomatic localization-related epilepsy caused by circumscribed cortical lesion were examined in the present study using 204-channel helmet-shaped MEG with a sampling rate of 600 Hz. One patient had dysembryoplastic neuroepithelial tumor (DNT) and three patients had focal cortical dysplasia (FCD). Aberrant areas were superimposed, to reconstruct 3D MRI images, and illustrated as moving images.
Results: In three patients, short-time Fourier transform (STFT) analyses of MEG showed rhythmic activities just above the lesion with FCD and in the vicinity of DNT. In one patient with FCD in the medial temporal lobe, rhythmic activity appeared in the ipsilateral frontal lobe and temporal lateral aspect. These findings correlate well with the results obtained by intraoperative electrocorticography. After the surgery, three patients were relieved of their seizures, and the area of rhythmic MEG activity disappeared or become smaller. One patient had residual rhythmic MEG activity, and she suffered from seizure relapse.

* Corresponding author. Tel.: +81 11 706 5954; fax: +81 11 706 7898.
E-mail address: ss11@med.hokudai.ac.jp (S. Saitoh).

0920-1211/$ – see front matter
doi:10.1016/j.eplepsyres.2009.10.002

Conclusion: Time–frequency analyses using STFT successfully depicted MEG rhythmic fast activity, and would provide valuable information for pre- and post-surgical evaluations to define surgical strategies for patients with epilepsy.

Introduction

Magnetoencephalography (MEG) is applied to localize the source of epileptiform discharges in patients with refractory epilepsy, particularly in symptomatic localization-related epilepsy, as it is noninvasive and exhibits excellent temporal and spatial resolution. MEG is a predictive tool for epileptic surgery. MEG localization of epileptiform discharges has been successfully achieved by single dipole modeling (SDM), which is mainly used to analyze interictal epileptiform spikes (Hämäläinen et al., 1993; Ebersol, 1997). However, the application of SDM appears to be limited to patients with localized spikes, since the algorithm is based on the presumption that the current epileptic discharge originates from a single spot.

Rhythmic electroencephalography (EEG) activities are often the hallmarks of underlying epileptogenesis. Rhythmic polyspike activities have been reported as indicative of an irritative epileptogenic zone in the electroencephalography (Gambardella et al., 1996). A scalp EEG showed interictal focal paroxysmal beta activity in children with epilepsy caused by brain tumor, arteriovenous malformation, and cystic lesion (Hooshmand et al., 1980). In surveys of surgical outcomes, the locations of ictal rhythmic beta activities on scalp EEG and intracranial EEG have been correlated with the onset of seizures in patients with neocortical epilepsies (Talairach et al., 1992; Lee et al., 2000; Park et al., 2002; Worrell et al., 2002; Bonati et al., 2006). However, the resolution of EEG is not powerful enough to properly evaluate rhythmic activity because EEG activity is affected by the conductivity of brain structures (Hämäläinen et al., 1993), and in some cases EEG is unable to detect notable pathological activity (Iwasaki et al., 2005).

Recently, time–frequency analyses of EEG and MEG have been used to investigate rhythmic activities (Haykin et al., 1996; Grosse et al., 2002; Bosnyakova et al., 2006). Short-time Fourier transform (STFT) applies a short-time window to the signal and performs a series of Fourier transforms within this window as it slides across the recorded data (Oppenheim and Schafer, 1999). This technique can be used to estimate the time–frequency components of the signal and visualize the spectral distributions. It has been proposed to apply this technique to patients with epilepsy (Kiymik et al., 2005), as it provides temporal changing information on the time–frequency domain.

Our current study was conducted to evaluate the effectiveness of surgery for epilepsy using pre- and post-operative MEG to assess changes in epileptic rhythmic activity.

Patients and methods

Patients

Four children with refractory symptomatic localization-related epilepsy induced by a circumscribed cortical lesion were enrolled in the present study. They underwent surgery between September 2005 and April 2008. Their guardians gave written informed consent for this study.

Methods

MEG

MEG data before and after surgery were recorded using a 204-channel helmet-shaped neuromagnetometer (Neuromag Vectorview; Elekta-Neuromag Oy, Stockholm, Sweden) with pairs of orthogonal planar gradiometers at 102 locations. The recordings were carried out in a magnetically shielded room, with the patient in a supine position. The MEG data were collected for about 40 min for each patient at a sampling rate of 600 Hz. During the MEG examination, Patients 1, 2 and 4 received intravenous sodium thiopental for sedation, to avoid motion artifacts, while Patient 3 did not require sedation. A scalp EEG was recorded simultaneously using the international 10-20 system.

MEG data analysis. MEG data were filtered for offline analysis with a band pass of 3–100 Hz.

The segments that contained abnormal paroxysms were selected manually. Single spikes were analyzed by SDM, to determine the distribution of brain activity generating the spike. Rhythmic fast activity discharges were analyzed by STFT, to determine the localization and value of each selected discharge.

SDM. The dipole-fit software (Neuromag, Helsinki, Finland) was used to calculate the equivalent current dipoles (ECDs). We defined acceptable ECDs as having goodness of fit (GOF) >70% and ECD strength of between 100 and 800 nAm. GOF is a measure of how well the ECD model explains the measured signals. Acceptable ECDs were superimposed on the MRIs.

STFT analysis. STFT was used to reveal the distributions of MEG fast activity (Oppenheim and Schafer, 1999) and the MATLAB (MathWorks, Natick, MA, USA) program was used to execute the STFT for the MEG signals. Each signal was divided into small sequential frames, and fast Fourier transformation (FFT) was applied to each frame.

In the present study, the STFT was implemented using a 256-point window. The time of each window was 426.7 ms (i.e., 256 points × 1000 ms/600 Hz). The window was shifted every four points, which corresponded to 6.7 ms (i.e., 1000 ms/600 Hz × 4 points). FFT was applied to each window. This process was repeated for the whole signals that were selected. The time–frequency distributions are displayed as graphs (Fig. 2C).

A spectrum was considered to be aberrant when it was observed in the graph to be isolated from the background frequency spectrum. An aberrant frequency spectrum on the graph was superimposed onto the reconstructed 3D MRI.

ECoG

The ECoG studies were performed during surgery. The ECoG data were collected using the Ceegraph system (Bio-Logic, Mundelein, IL, USA), with a sampling rate of 512 Hz. A 4 × 5 grid electrode array was used for Patients 1 and 4. A 4 × 8 grid electrode array was used for Patient 3. A four-channel strip electrode was used for Patient 2. Recording was performed for at least 1 min at each electrode location.

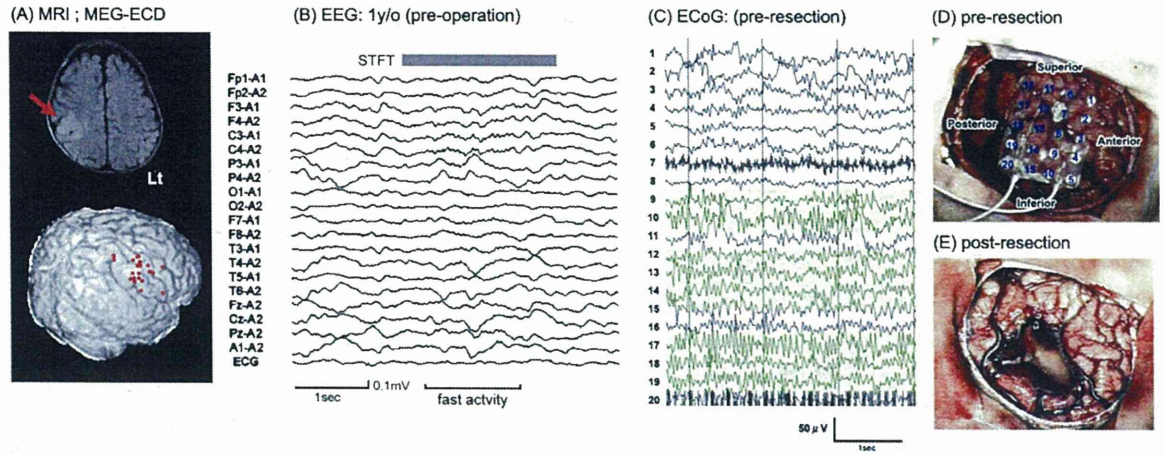

Figure 1 (A) Top panel: FLAIR MRI showing FCD on right parietal–occipital areas. Bottom panel: ECDs located at the FCD (red dot). (B) EEG at 1 year of age, just before the operation, demonstrating fast activity discharges at electrode C3, C4 interictally. (C) ECoG during operation before resection of lesion indicates 18–22-Hz polyspike bursts at electrodes 9, 10, 12–15, 17, 18, and 19 (yellow bar). These electrodes are located on top of the FCD. (D) FCD was exposed at the right supra-marginal gyrus during the operation. (E) FCD was resected after the operation. (For interpretation of the references to color in this figure legend, the reader is referred to the web version of the article.)

MRI

MRI was acquired with a 1.5 T high-resolution MRI scanner (Magnetom VISION; Siemens AG, Erlangen, Germany) for both diagnostic purposes and co-registration with the MEG data. Axial T1-weighted images (WI), T2WI, fluid-attenuated inversion recovery (FLAIR) images, and gadolinium-enhanced T1WI were obtained.

Single-photon emission computed tomography (SPECT)

^{99m}Tc L-ethyl cysteinate dimer (^{99m}Tc-ECD)-SPECT was performed interictally and ictally for Patient 2, and interictally for Patient 3. We used a ring-type SPECT scanner (Headtome-SET070; Shimadzu Corp., Kyoto, Japan). The ^{99m}Tc-ECD was injected intravenously at a dose of 111 MBq into Patient 2 and at 600 MBq into Patient 3.

Positron emission tomography (PET)

^{18}F-Fluorodeoxyglucose (FDG)-PET and ^{11}C-flumazenil (FMZ)-PET were performed for Patient 2 using the EXACT ECAT HR+ head scanner (Siemens). The injected doses of ^{18}F-FDG and ^{11}C-FMZ were 185 MBq and 370 MBq, respectively.

Results

Case reports

Patient 1

A 17-month-old boy had daily seizures. At 1 month of age, he began to have daily seizures with loss of consciousness and tonic extension of bilateral upper limbs. His seizure was refractory to various anti-epileptic drugs. Initially, his MRI finding was normal. At 16 months of age, a circumscribed lesion appeared on MRI with low intensity in the T1WI, high intensity in the T2WI, and FLAIR in right supra-marginal gyrus (Fig. 1A). An interictal EEG revealed rare spikes at electrodes C4 and P4 and low-voltage 10–12-Hz fast activity at electrodes C3 and C4 (Fig. 1B).

The 204ch MEG corresponding to the EEG fast activity showed rhythmic activities in the right central temporal areas (Fig. 2A). The ECDs were scattered over the cortical lesion (Fig. 1A, bottom panel). STFT analysis indicated a specific aberrant 15–18-Hz oscillation in the right central temporal areas (Fig. 2C). The specific oscillation at 15–18 Hz was generated at the focal cortical dysplasia (FCD) in the moving image (Fig. 3A).

The patient underwent craniotomy at 18 months of age. Intraoperative ECoG showed 18–19-Hz polyspike bursts at electrodes 9, 10, 12–15, 17, 18, and 19. These electrodes were located upon the resected cortical lesion (Fig. 1C, yellow bar). The frequencies of the MEG rhythmic activities (15–18 Hz) and ECoG polyspike (18–22 Hz) were comparable, and the locations of the MEG and ECoG oscillation almost overlapped. A total lesionectomy was performed.

The pathology was focal cortical dysplasia with balloon cells (Palmini type 2B). The patient has remained seizure-free for 22 months and has developed steadily.

Patient 2

A 2-year-old girl had daily seizures. At age 10 months, she experienced an afebrile, generalized, tonic-clinic seizure. MRI showed a left frontal cortical construction anomaly. At 15 months of age, she began to have seizures with extension of her right arm and leg, flexion of her left arm and leg, and deviation of her head and eyes to the right. Although anti-epileptic drugs controlled the seizures, she was able to speak only a few words at 32 months of age.

T2WI and FLAIR MRI showed cortical thickening in the left frontal lobe, blurring of the gray-white matter junction and hyperintensity of the subcortical white matter. Interictal ^{99m}Tc-ECD-SPECT showed hypoperfusion in the left frontal area and ictal ^{99m}Tc-ECD-SPECT revealed hyperperfusion in the left frontal area. ^{18}F-FDG-PET showed hypometabolism in the left frontal area, and ^{11}C-FMZ PET demonstrated decreased binding at the left frontal area.

Interictal EEG demonstrated rhythmic, 13–14-Hz, low-voltage fast activity and a low number of sharp waves

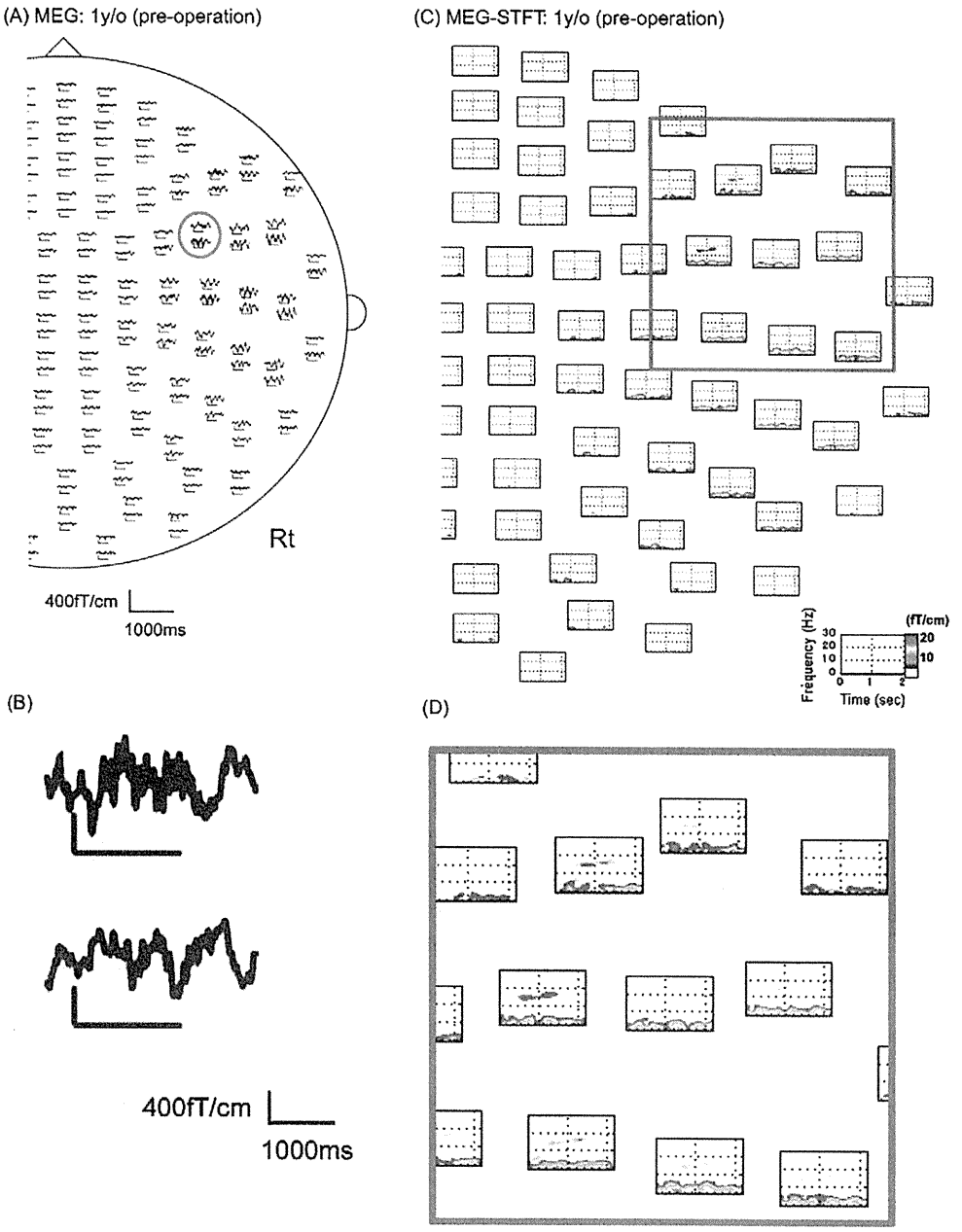

Figure 2 (A) 204ch MEG corresponding to interictal fast activity on the EEG (gray bar in Fig. 1B) demonstrates polyspikes at the right central temporal areas. (B) One representative gradiometer (red circle in (A)) showing rhythmic activity. (C) STFT graph showing specific rhythmic activities with 15–18-Hz oscillation at the right central temporal areas (red squire). (D) Enlarged section of red squire in (C). (For interpretation of the references to color in this figure legend, the reader is referred to the web version of the article.)

at electrodes Fp1, Fp2, F3, and F7. Ictal EEG showed desynchronization, followed by left frontal spikes and slow waves.

The 204ch MEG corresponding to the EEG fast activity showed rhythmic activities at the left frontal–temporal areas. The ECDs were not clustered due to the low number of isolated spikes with sufficient signal-to-noise ratio. STFT analysis indicated that a specific, aberrant, 15–20-Hz oscillation was generated at the left superior temporal gyrus and propagated to the middle and inferior frontal gyri in the moving image (Fig. 3B, top panel).

The patient underwent the operation at 36 months. Intraoperative ECoG showed 13–25-Hz spikes and polyspikes at the orbito-frontal area.

The frequencies of the MEG oscillation (15–20 Hz) and ECoG polyspike (13–25 Hz) were comparable. ECoG polyspikes were located inside the area where the MEG oscillation was depicted by moving images.

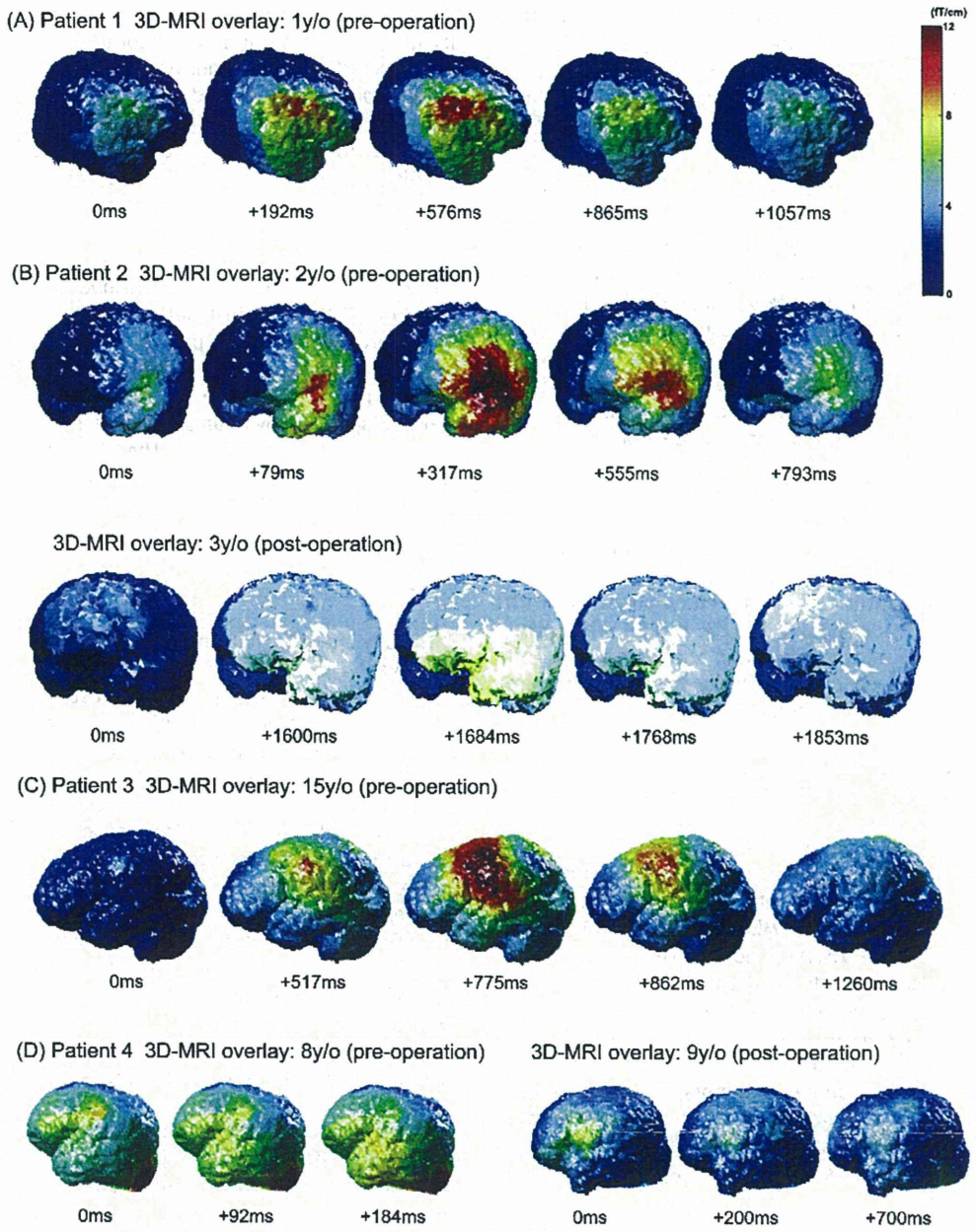

Figure 3 (A) Specific oscillation at 15–18 Hz generated at the FCD in the superimposed 3D MRI image of Fig. 2C in Patient 1. (B) Top panel: Preoperative superimposed 3D MRI image in Patient 2 showing specific oscillation generated at the superior temporal, middle-frontal gyrus, and inferior frontal gyrus. Bottom panel: Post-operative superimposed 3D MRI image in Patient 2 showing specific oscillation generated at the superior temporal, middle-frontal gyrus, and inferior frontal gyrus. (C) Superimposed 3D MRI image in Patient 3 showing specific oscillation generated in the vicinity of the DNT. (D) Left panel: Preoperative superimposed 3D MRI image in Patient 4 showing broad aberrant oscillation at the left lateral occipital lobe, at the inferior, middle, and superior temporal gyrus, at the angular gyrus, supra-marginal gyrus and the inferior frontal gyrus (red and yellow areas). Right panel: Post-operative superimposed 3D MRI image in Patient 4 showing broad aberrant oscillation at the left angular gyrus and at the inferior frontal gyrus (yellow area). (For interpretation of the references to color in this figure legend, the reader is referred to the web version of the article.)

Based on the FDG-PET findings, the patient underwent left frontal lobe disconnection. The pathology was FCD with dysmorphic neuron and without balloon cells (Palmini type 2A). The patient had remained seizure-free for 8 months and her development improved dramatically.

At age 44 months, 8 months after operation, interictal EEG demonstrated spikes at electrodes Fp1, F3, F7 and fragment polyspikes at electrode F7. The MEG showed residual rhythmic activities at the left frontal–temporal areas. STFT analysis of the moving image indicated that a specific, aber-

rant, 15–20-Hz oscillation was generated at the left superior temporal (Fig. 3B, bottom panel). Subsequently, she had seizure relapse. The ECDs were clustered at the left pars opercularis. Additional resection of the left pars opercularis was performed. The patient has since remained seizure-free for 8 months.

Patient 3

A 15-year-old girl had weekly, but sometimes daily, clusters of seizures. Her development was normal. At 6 years of age, she began to have weekly seizures with deviation of the eyes without loss of consciousness. At 10 years of age, she began to have the sensation of being in an elevator that was falling. Following the aura her head and eyes deviated to the right with loss of consciousness, and in some instances her seizure evolved into right-side clonic seizures. At 14 years of age, the first MRI showed a circumscribed mass of low intensity on T1WI and high intensity on T2WI in the left parietal–occipital regions.

Interictal ^{99m}Tc-ECD-SPECT showed hypoperfusion at the left parietal–occipital areas, which corresponded with the lesion found on MRI. Interictal EEG revealed polyspikes with slow waves at electrodes F3, F4, F7, C3, and C4. The corresponding 204ch MEG showed rhythmic activities in the left frontal and central areas. The ECDs for these spikes were scattered in the anterior vicinity of the MRI lesion. STFT analysis indicated a specific aberrant 20–25-Hz oscillation in the left frontal and central areas. The specific oscillation at 20–25 Hz was generated in the vicinity of the lesion in the moving images (Fig. 3C).

She underwent craniotomy at 16 years of age. The intraoperative ECoG showed 18–25-Hz polyspike bursts at electrodes which were located at the anterior vicinity of the lesion. The frequencies of the MEG oscillation (20–25 Hz) and ECoG polyspike (18–25 Hz) almost corresponded. ECoG polyspikes were located inside the area where the MEG oscillation was depicted by moving images. A total lesionectomy was carried out; the tumor and the gyri involved by the tumor were resected simultaneously.

The tumor was diagnosed as dysembryoplastic neuroepithelial tumor (DNT). One month after the operation, her EEG and MEG showed no fast activity. The patient has been seizure-free for 24 months post-surgery and exhibited no neurological deficits.

Patient 4

A 9-year-old girl had daily seizures. Her seizures initially occurred at 1 month of age with complex partial seizure with motion arrest, loss of consciousness and cyanotic change. Her seizures evolved to daily simple seizures, described as ictal fear and cephalic sensation, and complex partial seizures with motion arrest and autonomic change (cyanotic face) for 3–4 min without remarkable description of dystonic posturing. At 7 years of age, a circumscribed lesion appeared on the MRI in the T1WI at low intensity, in the T2WI and FLAIR at high intensity, in the left temporal parahippocampal gyrus, uncus and hippocampus. At 8 years of age, an EEG performed just before her operation showed independent spikes at the right occipital and left frontal areas, but these were not as intense in the left temporal area where the lesion existed. Furthermore, EEG and MEG showed intermittent, but prolonged, rhythmic activity at the left frontal and temporal areas. STFT analysis of rhythmic MEG activity during the pre- and post-operative periods demonstrated widespread rhythmic activity in the ipsilateral frontal lobe and in the lateral aspect of the temporal lobe (Fig. 3D, left panel). This rhythmic activity disappeared after the operation and became localized to the left pre- and post-central gyrus (Fig. 3D, right panel).

She underwent an operation at 8 years of age. The intraoperative ECoG showed continuous rhythmic spikes at approximately 20 Hz just before dysplasia resection at the lower area of the left pre- and post-central gyrus and the supra-marginal gyrus. This activity disappeared and became restricted to the left pre-frontal gyrus and supra-marginal gyrus at lower amplitude. One month after surgery, STFT analysis indicated that the oscillation became more restricted and of lower power than in the preoperative MEG (Fig. 3E, right panel).

Discussion

This study indicate that time–frequency analyses using STFT can reveal the distributions of rhythmic fast activity on MEG. This method is useful for pre- and post-surgical evaluation. To improve outcomes from epileptic surgery, it is essential to define the precise location of the epileptogenic zone and the margin of surgical resection by the pre-surgical evaluation. For these purposes, MEG analysis is considered to be a suitable technique, as it offers good temporal and spatial resolution and noninvasive.

We used thiopental for three of the four patients. Thiopental produces fast activity in the beta range (12–30 Hz). However, these fast activities are bilaterally symmetric and developed in a frontal–central area, similar to those appearing during drowsiness (Feshchenko et al., 1997, 2004). The fast activity in our study was generated unilaterally and not in a frontal–central area, thus the fast activity in our study was not attributed to thiopental.

Single dipole modeling has been used mainly to analyze the interictal epileptiform spikes on MEG. Oishi et al. (2006) reported that single clusters of ECDs indicated discrete epileptogenic zones that required complete resection for seizure-free outcome. In the present study, isolated interictal spikes were scarce in Patients 1 and 3, and the ECDs of Patients 1 and 3 were also scattered but not cluster. These ECDs were almost concordant with the high-power area of MEG fast activities, indicating that the SDM localizations were also useful for pre-surgical evaluation in these patients. In contrast, Patient 2 showed few ECDs, due to a scarcity of isolated spikes with sufficient signal-to-noise ratio. The ECDs in Patient 4 were clustered at two remote areas from epileptogenic area at left temporal lobe. These ECDs were discrete from the high-power area of MEG fast activities. ECDs might thereby reflect propagation from the source oscillation. The data obtained from the SDM were, therefore, insufficient for pre-surgical evaluation in our patients.

Ochi et al. (2007) used ECoG to investigate high frequency oscillation (HFO) at the epileptogenic focus and to assess the relationship between the outcome of surgery for epilepsy

and the pattern of HFO. Their findings demonstrated the significant value of preoperative analysis of rhythmic activity. MEG provides higher temporal resolution than EEG and was thus able to show epileptiform discharges more clearly than EEG. For this reason, MEG has the potential to more precisely analyze epileptic rhythmic discharges.

There were several advantages of the MEG findings for pre-surgical evaluation. In our study, epileptic rhythmic activity was demonstrated more clearly by MEG in all patients. Furthermore, the frequency of oscillation appeared faster by MEG than by EEG. For Patients 1, 2, and 4, the EEG showed bilateral fast activity. For Patient 3, EEG showed only a spike or polyspike and a slow wave complex that corresponded to the MEG fast activity. For Patient 2, who was nonlesional on MRI, STFT analysis indicated the epileptic foci, and together with the FDG-PET findings, this information enabled us to plan the disconnection strategy for surgery. For Patient 3, the data enabled us to place the intraoperative ECoG electrodes not only on the lesion, but also at the anterior vicinity of the lesion and source of the fast activity. Similarly, the STFT findings for Patient 4, facilitated placing the ECoG electrodes. STFT analysis of fast activity is thus clearly beneficial for predicting the epileptic foci in patients with poor or several ECDs and for placing the ECoG electrodes.

Our study analyzed the changes in epileptic rhythmic activity before and after surgery for epilepsy and demonstrated the clinical value in predicting the outcome of surgery. For Patient 3, the MEG polyspikes and spikes disappeared following surgery and the patient became seizure-free. For Patients 2 and 4, especially, an aberrant rhythmic oscillation appeared in the remote area of the primary epileptic focus: FCD or DNT. For Patient 4, this rhythmic activity disappeared after the operation. For Patient 2, the MEG polyspikes persisted after surgery and her seizures relapsed. This remote rhythmic activity was defined as secondary epileptogenic focus. In some cases a supplementary operation, such as multiple sub-pial transection, is conducted to treat the secondary focus. Our operative strategy was lesionectomy and we planned further resection according to the seizure outcome and outcome of MEG after the operation. Post-operative MEG showing normal or notably improved aberrant rhythmic oscillation suggests a favorable outcome, whereas post-surgical residual MEG polyspikes may indicate a risk of seizure relapse. Our findings from MEG correlated with seizure outcome. Thus, MEG provides a useful post-surgical evaluation procedure to indicate the need for a secondary operation. In this way, MEG avoids redundant resection and is a safe and noninvasive procedure.

Concerning the correlation between the MEG and ECoG findings, the high-power area of MEG fast activity for Patient 1with FCD (shown in the red area of the 3D movie; Fig. 3A) and the area of ECoG polyspikes were consistent, with both oscillations colocalizing at the FCD. For Patient 2 with FCD, the ECoG polyspikes were located within the high-power area of MEG fast activity (shown in the red area of the 3D movie; Fig. 3B). For Patient 3 with DNT, the ECoG polyspikes were within the high-power area of MEG fast activity (shown in the red area of the 3D movie; Fig. 3C), and both areas were located near the tumor. For Patient 4 with FCD, the high-power area of MEG fast activity (shown in the yellow area of the 3D movie; Fig. 3D, left panel) was consistent with the area of ECoG polyspikes. Thus, the MEG fast activity locations demonstrated by STFT colocalized well with the ECoG polyspikes in patients, while MEG areas were rather wider. This could be due to the distance (several cm) between the cortical surface and the MEG sensors, the size of the planar gradiometer sensor, and the distance between sensors.

Guggisberg et al. (2008) showed the clinical value of MEG for the epileptic rhythmic activities in correlation with ECoG. Consistent with the results of previous studies, our findings suggest that STFT of MEG data can depict fast activity that indicate epileptogenic zones associated with FCD and DNT, which are the most significant etiologies of pediatric intractable symptomatic localization-related epilepsy. The excellent post-surgical outcomes achieved for our patients strongly support the predictive value of noninvasive MEG analysis. The rhythmic activities that are closely correlated to the ictogenesis in the cerebral cortex can be demonstrated stereoscopically by noninvasive MEG.

This STFT analysis is limited to patients who have aberrant frequency oscillation like fast activity in our study isolated from the background frequency spectrum. However, unlike ECD and other spatial filtering methods, STFT confers the following advantages. (1) STFT analyzed the original recorded magnetic field data directly. (2) Parameters do not need to be selected arbitrarily to make assumptions about current source and volume conductor, and thus to solve the inverse problem for source localization. (3) STFT indicates the temporal changes. (4) STFT can analyze oscillations that are generated simultaneously over a wide area and with low signal-to-noise ratio.

On the other hand, there were some limitations of this study. First, because the planar gradiometers evaluate the magnetic field just beneath the sensor, STFT could not reflect the depth of source. Second, because of the sensor size of planar gradiometer are 2.8 cm × 2.8 cm and distance between sensor centers is 3.4 cm, there might be a 1–2 cm errors between oscillation sources and projected position of sensor on 3D MRI.

In conclusion, MEG can detect fast activity in symptomatic localized-related epilepsy more clearly and accurately than conventional EEG. STFT reveal the frequency and location of MEG fast activity that could not be analyzed by SDM. The MEG fast activity findings correlated well with the intraoperative ECoG findings and are therefore useful for pre-surgical evaluation. Ascertaining the presence of fast activity after epilepsy surgery could predict the prognosis of seizures. This noninvasive evaluation provides valuable information for pre- and post-surgical evaluations to define surgical strategies for patients with symptomatic localization-related epilepsy induced by circumscribed cortical lesions.

Conflicts of interest

None of the authors has any conflict of interest to disclose.

Acknowledgments

We thank Prof. Tadashi Ariga of the Department of Pediatrics, Hokkaido University Graduate School of Medicine,

for his valuable editorial opinion. In addition, we thank Dr. Akiyoshi Kakita of the Brain Research Institute, Niigata University for pathology diagnoses. We confirm that we have read the Journal's position on issues involved in ethical publication and affirm that this report is consistent with those guidelines. This work was supported in part by Grants-in-aid for Scientific Research (18591136) from the Japan Society of the Promotion of Science, and the Japan Epilepsy Research Foundation.

References

Bonati, L.H., Naegelin, Y., Wieser, H.G., Fuhr, P., Rueqq, S., 2006. Beta activity in status epilepticus. Epilepsia 47, 207–210.

Bosnyakova, D., Gabova, A., Kuznetsova, G., Obukhov, Y., Midzyanovskaya, I., Salonin, D., van Rijn, C., Coenen, A., Tuomisto, L., van Luijtelaar, G., 2006. Time–frequency analysis of spike-wave discharges using a modified wavelet transform. J. Neurosci. Methods 154, 80–88.

Ebersol, J.S., 1997. Magnetoencephalography/magnetic source imaging in the assessment of patients with epilepsy. Epilepsia 38 (Suppl. 4), S1–S5.

Feshchenko, V.A., Veselis, R.A., Reinsel, R.A., 1997. Comparison of the EEG effects of midazolam, thiopental, and propofol: the role of underlying oscillatory systems. Neuropsychobiology 35, 211–220.

Feshchenko, V.A., Veselis, R.A., Reinsel, R.A., 2004. Propofol-induced alpha rhythm. Neuropsychobiology 50, 257–266.

Gambardella, A., Palmini, A., Andermann, F., Dubeau, F., Da Costa, J.C., Quesney, L.E., Andermann, E., Livier, A., 1996. Usefulness of focal rhythmic discharges on scalp EEG of patients with focal cortical dysplasia and intractable epilepsy. Electroencephalogr. Clin. Neurophysiol. 98, 243–249.

Grosse, P., Cassidy, M.J., Brown, P., 2002. EEG-EMG, MEG-EMG and EMG-EMG frequency analysis: physiological principles and clinical applications. Clin. Neurophysiol. 113, 1523–1531.

Guggisberg, A.G., Kirsch, H.E., Mantle, M.M., Barbaro, N.M., Nagarajan, S.S., 2008. Fast oscillations associated with interictal spikes localize the epileptogenic zone in patients with partial epilepsy. Neuroimage 39, 661–668.

Hämäläinen, M.S., Hari, R., Ilmoniemi, R., Knuutila, J., Lounasmaa, O.V., 1993. Magnetoencephalography: theory, instrumentation, and applications to noninvasive studies of the working human brain. Rev. Mod. Phys. 65, 413–497.

Haykin, S., Racine, R.J., Xu, Y., Chapman, C.A., 1996. Monitoring neuronal oscillations and signal transmissions between cortical regions using time–frequency analysis of electroencephalographic activity. Proc. IEEE 84, 1295–1301.

Hooshmand, H., Morganroth, R., Corredor, C., 1980. Significance of focal and lateralized beta activity in the EEG. Clin. Electroencephalogr. 11, 140–144.

Iwasaki, M., Pestana, E., Burgess, R.C., Lüders, H.O., Shamoto, H., Nakasato, N., 2005. Detection of epileptiform activity by human interpreters: blinded comparison between electroencephalography and magnetoencephalography. Epilepsia 46, 59–68.

Kiymik, M.K., Güler, I., Dizibüyük, A., Akin, M., 2005. Comparison of STFT and wavelet transform methods in determining epileptic seizure activity in EEG signals for real-time application. Comput. Biol. Med. 35, 603–616.

Lee, S.K., Kim, J.Y., Hong, K.S., Nam, H.W., Park, S.H., Chung, C.K., 2000. The clinical usefulness of ictal surface EEG in neocortical epilepsy. Epilepsia 41, 1450–1455.

Ochi, A., Otsubo, H., Donner, E.J., Elliott, I., Iwata, R., Funaki, T., Akizuki, Y., Akiyama, T., Imai, K., Rutka, J.T., Snead 3rd., O.C., 2007. Dynamic changes of ictal high-frequency oscillations in neocortical epilepsy: using multiple band frequency analysis. Epilepsia 48, 286–296.

Oishi, M., Kameyama, S., Masuda, H., Tohyama, J., Kanazawa, O., Sasagawa, M., Otsubo, H., 2006. Single and multiple clusters of magnetoencephalographic dipoles in neocortical epilepsy: significance in characterizing the epileptogenic zone. Epilepsia 47, 355–364.

Oppenheim, A., Schafer, R.W., 1999. Discrete-Time Signal Processing. Prentice Hall, Englewood Cliffs, New Jersey.

Park, S.A., Lim, S.R., Kim, G.S., Heo, K., Park, S.C., Chang, J.W., Chung, S.S., Choi, J.U., Kim, T.S., Lee, B.I., 2002. Ictal electrocorticographic findings related with surgical outcomes in nonlesional neocortical epilepsy. Epilepsy Res. 48, 199–206.

Talairach, J., Bancaud, J., Bonis, A., Szikla, G., Trottier, S., Vignal, J.P., Chauvel, P., Munari, C., Chodkievicz, J.P., 1992. Surgical therapy for frontal epilepsies. Adv. Neurol. 57, 707–732.

Worrell, G.A., So, E.L., Kazemi, J., O'Brien, T.J., Mosewich, R.K., Cascino, G.D., Meyer, F.B., Marsh, W.R., 2002. Focal ictal beta discharge on scalp EEG predicts excellent outcome of frontal lobe epilepsy surgery. Epilepsia 43, 277–282.

and 83%, respectively.[1] However, patients presenting with an advanced stage of adult WT still show a poor outcome. In a recent NWTS retrospective report, OS (with a mean observation time of 54 months) was only 20% for stage IV adult WT.[7]

The present patient initially presented with highly extensive disease, which was cured with multimodal therapy based on pediatric strategy. Because the patient's hematological toxicities were always serious, the interval between chemotherapy was thus prolonged. In addition, we also decided to use the minimum required radiation dosage and PBSC rescue. Furthermore, the patient's neurotoxicity secondary to vincristine was also serious, thus requiring the use of special equipment.

This case demonstrated that WT observed in the adolescent and adult population, even when identified at an advanced stage, appears to be curable if multimodal treatment according to the established pediatric strategy is effectively performed. However, toxicity such as hematological toxicity and neuropathy may develop at a higher incidence and at a more severe grade.[1,2] In this case the PBSC rescue may not have been needed, however this method should nevertheless be considered in patients presenting with severe hematological toxicity. Kalapurakal *et al.* pointed out the risk of veno-occlusive disease associated with an overdosage of ACD in adult patients.[2] Therefore, such toxicities should be closely monitored in adult patients with WT. Moreover, prospective trials in both adolescent and adult patients with WT are warranted in order to establish the appropriate dosages and optimal schedule of chemotherapy, as well as to determine the ideal sequence and effective design of local treatments and supportive care.

References

1 Reinhard H, Aliani S, Ruebe C *et al.* Wilms' tumor in adults: results of the Society of Pediatric Oncology (SIOP) 93-01/ Society for Pediatric Oncology and Hematology (GPOH) study. *J. Clin. Oncol.* 2004; **22**: 4500–6.
2 Kalapurakal JA, Nan B, Norkool P *et al.* Treatment outcomes in adults with favorable histologic type Wilms tumor. *Int. J. Radiat. Oncol. Biol. Phys.* 2004; **60**: 1379–84.
3 Arrigo S, Beckwith JB, Sharples K *et al.* Better survival after combined modality care for adults with Wilms' tumor. A report from National Wilms' Tumor Study. *Cancer* 1990; **66**: 827–30.
4 Kaste SC, Dome JS, Babyn PS *et al.* Wilms tumor: prognostic factors, staging, therapy and late effects. *Pediatr. Radiol.* 2008; **38**: 2–17.
5 Pizzo PA, Poplack DG, eds. *Principles and Practice of Pediatric Oncology*, 5th edn. Lipponcott Williams and Wilkins, Philadelphia, PA, 2006; 905–32.
6 Byrd RL, Evans AE, D'Angio GJ. Adult Wilms's tumor: effect of combined therapy on survival. *J. Urol.* **982**(27): 648–51.
7 Izawa JI, Al-Omar M, Winquist E *et al.* Prognostic variables in adult Wilms tumor. *Can. J. Surg.* 2008; **51**: 252–6.

Vaccine-associated paralytic poliomyelitis in a non-immunocompromised infant

Naoko Asahina,[1] Yukiko Matsunami,[2] Keitaro Sueda,[1] Hideaki Shiraishi[1] and Shinji Saitoh[1]

[1]*Department of Pediatrics, Hokkaido University Graduate School of Medicine and* [2]*Department of Pediatrics, KKR Sapporo Medical Center, Sapporo, Japan*

Key words oral poliovirus vaccine, poliomyelitis, primary immunodeficiencies, tissue injury, vaccine-associated paralytic poliomyelitis.

Oral poliovirus vaccine (OPV) was introduced in Japan in 1961 and it has become a routine immunization for infants since 1964. During the 1960s, the widespread use of OPV led to a dramatic decrease in the number of patients contracting poliomyelitis. Since 1981, no poliomyelitis cases caused by wild poliovirus have been reported in Japan.[1] Live virus vaccination, however, is associated with the serious consequence of vaccine-associated paralytic poliomyelitis (VAPP). In 2002, the World Health Organization estimated that between 250 and 500 cases of VAPP occur every year due to the use of OPV in routine childhood immunization programs around the world.[2] Although VAPP can occur in healthy recipients or their close contacts, persons with primary immunodeficiencies have a much higher risk of the disease.[3,4]

In Japan, the overall risk for recipient and contact VAPP has been reported as one case in every 2 million doses given, while the risk of recipient VAPP and recipient VAPP following the first OPV dose is one in every 3.7 million doses and one in every 2.3 million doses given, respectively.[5]

In this study, we report a case of VAPP in an infant who did not have any obvious immunodeficiency.

Correspondence: Shinji Saitoh, MD PhD, Department of Pediatrics, Hokkaido University Graduate School of Medicine, North 15, West 7, Kita-ku, Sapporo 060-8638, Japan. Email: ss11@med.hokudai.ac.jp

Received 23 May 2009; revised 8 January 2010; accepted 29 January 2010.
doi: 10.1111/j.1442-200X.2010.03132.x

Case report

A 7-month-old male infant of healthy parents was presented with a high fever of 39°C and a perianal abscess, 15 days after his first